JOURNAL OF APPLIED ELECTROCHEMISTRY 20 (1990) 1009–1014

Zinc deposition and passivated hydrogen evolution in highly acidic sulphate electrolytes: depassivation by nickel impurities

C. CACHET, R. WIART

LP 15 du CNRS 'Physique des Liquides et Electrochimie', Laboratoire de l'Université Pierre et Marie Curie, Tour 22–4, Place Jussieu, 75252 Paris, Cédex 05, France

Received 6 December 1989; revised 25 April 1990

In highly acidic sulphate electrolytes used for zinc electrowinning, the steady-state behaviour and the impedance of zinc electrodes have been analyzed under potentiostatic control. It is shown that zinc deposition takes place under conditions where hydrogen evolution remains passivated on the deposit surface. A depassivation of hydrogen evolution leading to the deposit corrosion can be provoked by an electrode excursion near the corrosion potential. The presence of nickel impurities facilitates this depassivation process even though the electrode potential remains cathodic. The depassivation becomes easier with the existence of a scratch on the substrate surface, because of bubbles retained on this defect.

1. Introduction

For zinc deposition in slightly acidic electrolytes, S-shaped polarization curves have been reported [1, 2] with the existence of three different cathodic current densities at some electrode potentials. It has been shown that these multiple steady-states can be eliminated by decreasing the pH, and a clear inhibition of zinc deposition has been observed in highly acidic sulphate solutions [2]. The strong interactions between the H^+ and Zn^{2+} discharges have been described by a model involving several elementary steps, and based on a competition between the autocatalytic production of the adsorbed intermediate Zn^+_{ads} according to the reaction ($Zn^{2+} + Zn^+_{ads} + e^- \rightleftharpoons 2Zn^+_{ads}$) and the adsorption of H_{ads} acting primarily as an inhibitor for zinc deposition. The current dependencies of both the surface coverages by these adsorbates and the surface concentration of active sites for zinc deposition account for the three time constants of the inductive faradaic impedance apparent at various current densities along the S-shaped polarization curves.

In highly acidic sulphate electrolytes used in zinc electrometallurgy, the kinetics of zinc electrodeposition have been extensively investigated on the basis of electron microscopy, cyclic voltammetry and current efficiency [3–7]. It has been shown that the hydrogen discharge reaction is inhibited by the presence of Zn^{2+} ions in the electrolyte [5] and that the hydrogen evolution current is activated by the presence of nickel impurities in the electrolyte [5]. The voltammograms, obtained with aluminium electrodes covered by relatively thin zinc deposits, remain sensitive to substrate impurities which possibly stimulate hydrogen evolution [7], and also sensitive to the grain size of the substrate which considerably influences zinc nucleation [6]. It is during the growth of thick deposits from nickel-containing electrolytes that the zinc deposition process has been observed to destabilize and degenerate into zinc corrosion and hydrogen evolution, after a time lapse which defines the induction period. So it appears of interest to investigate the mechanism of the slow formation of thick zinc deposits under steady-state quasi steady-state conditions, as a substrate-independent process.

Impedance measurements have been recently performed during the galvanostatic deposition of zinc under various hydrodynamic conditions [8]. The electrode impedance has been shown to be significantly modified when zinc deposition is destabilized in the presence of nickel impurities, and such a change in the electrode behaviour occurs simultaneously with a decrease in the cathodic polarization, thus suggesting the possible existence of multiple steady-states of the electrode.

Aiming at a better knowledge of the cathodic processes taking place on the zinc electrode in highly acidic sulphate electrolytes, the steady-state behaviour and the impedance of zinc electrodes have been analyzed for various time-lapses and various additions of nickel ions. The results of this experimental investigation are presented and discussed in the present paper.

2. Experimental details

The solution was made of $55\,g\,l^{-1}$ zinc from $ZnSO_4$, $7H_2O$ and $120\,g\,l^{-1}$ H_2SO_4. To this solution, nickel was added as $NiSO_4$, $6H_2O$ at concentrations (between 0.1 and $90\,mg\,l^{-1}$) often higher than levels encountered in industrial solutions. All chemicals were Merck pro-analysis products and the water was doubly ion-

0021-891X/90 $03.00 + .12

exchanged and twice distilled in a quartz apparatus. The counter electrode was a platinum gauze cylinder and potentials were referred to a mercury/mercurous sulphate electrode in saturated potassium sulphate (SSE), used with two compartments separated by fritted glass. The working electrode was fashioned from a 0.5 cm diameter zinc cylinder (Johnson–Matthey 99.999%) the lateral wall of which was insulated with epoxide resin (Buehler). It was fitted either as a classical rotating disc electrode or as a stationary electrode whose effective surface (0.2 cm^2 area) was vertical and parallel to the symmetry axis of the cell. Before electrolysis, the zinc electrode was polished with emery paper (1200 grade). The cell temperature was maintained at 36° C. In view of the $ZnSO_4$ purity, the maximum levels of impurities contained in electrolytes were: K, Na, Ca, Pb 8 × 10^{-6} M; Mn 3 × 10^{-6} M; N, Cl, Cu, Fe, Cd 4 × 10^{-6} M, As 8.4 × 10^{-7} M. In some experiments, a preelectrolysis was performed so as to eliminate at least 99% of metal impurities which were deposited at −1.5 V with respect to SSE.

Steady-state polarization curves were obtained potentiostatically: after 1 h deposition at a constant polarization chosen between −1.52 and −1.54 V, all curves were obtained by stepping the potential and waiting for the current stabilization at each potential. Impedance measurements were performed using a frequency response analyser (Solartron 1174) controlled by an Apple II microcomputer. All polarization curves were corrected for the ohmic drop due to the electrolyte resistance of 0.4 Ω cm^{-2}.

3. Results and discussion

3.1. *Nickel-free electrolytes*

The steady-state polarization curves recorded under potentiostatic conditions with a rotating disc electrode are depicted in Fig. 1. Starting from point S, the steady-state polarization curve 1 can be recorded with a fresh electrolyte with both decreasing and increasing polarization between −1.53 and −1.40 V/SSE. Over a large range of potential (−1.4 to −1.5 V), practically no current exists and the electrode seems to be blocked in a way similar to that already reported in sulphate electrolyte [8]. However, after using the electrolyte for about 12 h, decreasing the electrode polarization from point S reveals a small peak (at −1.42 V on curve 2) corresponding to a progressive electrode activation. After a stay at −1.4 V or at a more anodic potential, a hysteresis effect is observed with increasing polarization: the cathodic current values are higher than with decreasing polarization and an intense gas evolution is observed around the cathodic peak. Such a current peak was also obtained with an electrode directly polarized to −1.4 V. Curve 2 can be reproduced after a preelectrolysis eliminating 99% of lead, the main impurity able to increase the hydrogen evolution overvoltage on a zinc electrode [9]. Consequently this impurity in the electrolyte explains neither the hysteresis effect nor the electrode passivation, but only acts as a minor factor in the initial electrode blocking.

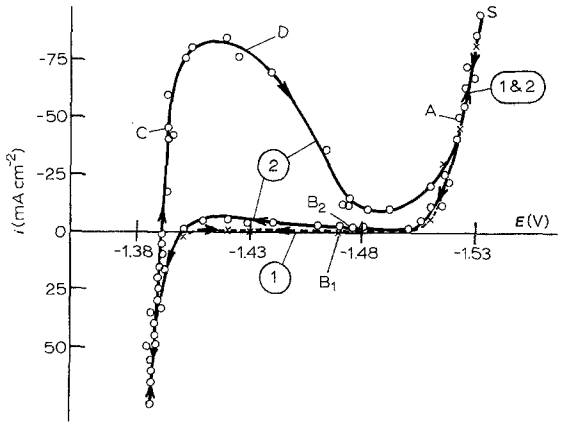

Fig. 1. Potentiostatic polarization curves in the electrolyte (120 g l^{-1} H_2SO_4, 55 g l^{-1} Zn^{2+}). Curve 1 (x): fresh electrolyte; curve 2 (O): after electrolysis for 12 h. Rotating disc electode, Ω = 2500 rpm. The arrows on curves indicate the direction of potential variation.

The steepness of the curve near the corrosion potential (−1.39 V) indicates a strong electrode activation due to the corrosion process, which releases the inhibiting adsorbates from the electrode surface. Then around the corrosion potential, the cathodic process corresponds to hydrogen evolution on an inhibitor-free electrode surface. With increasing cathodic polarization from the corrosion potential, the sharp cathodic peak is followed by a decrease in current due to the electrode passivation for hydrogen evolution, by inhibiting adsorbed species involved in zinc deposition. As soon as the inhibition of hydrogen evolution is achieved, curve 2 rejoins curve 1 at high cathodic potentials where zinc deposition takes place.

Different typical impedance plots obtained at various polarization points of Fig. 1 are shown in Fig. 2. Diagram A of Fig. 2 was obtained in the cathodic branch where zinc deposition takes place. The high frequency capacitive loop corresponds to the double layer capacitance in parallel with the charge transfer resistance. At frequencies below 30 Hz approximately, the electrode impedance is inductive and characterized by three time constants. With reference to previous works [1, 8] two of these loops correspond to the relaxation of the electrode coverages by the adsorbed species Zn^+_{ads} and H_{ads}, and the third loop, characterized by a much lower proper frequency (< 6 mHz), can be interpreted in terms of a slow electrode activation with increasing cathodic polarization [2]. In addition, the steepness of the cathodic branch of the current potential curve and the low value of the extrapolated polarization resistance indicate a sharp electrode activation with cathodic polarization similar to that already reported for zinc deposition in less acidic electrolytes [1, 2]. Such an electrode activation, necessary for zinc deposition to occur, is consistent with a strong inhibiting effect at potentials ranging between −1.4 and −1.5 V. This inhibition process also appears on diagram B_1: the inductive feature has disappeared and the electrode impedance remains

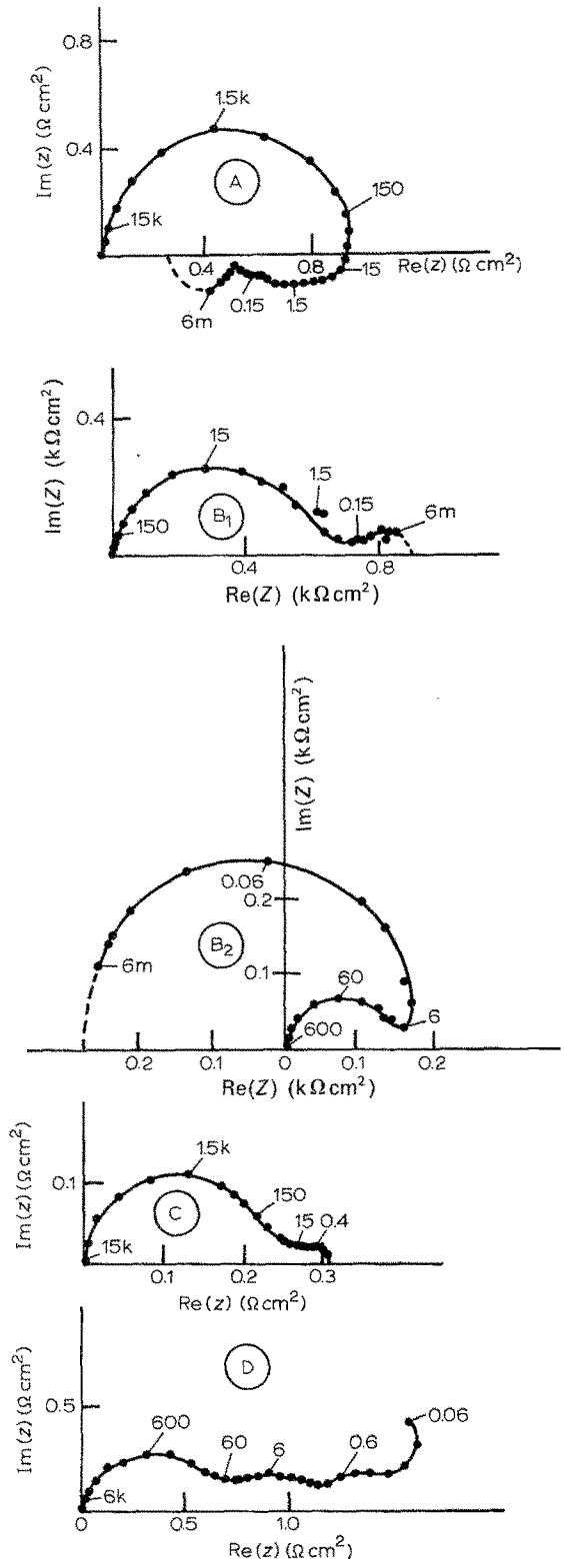

Fig. 2. Complex plane impedance plots obtained at points A, B_1, B_2, C and D in Fig. 1. Frequencies in Hz.

capacitive in the whole frequency domain. The high frequency capacitive loop reveals both an increase in the transfer resistance in agreement with slower reactions, and a decrease in the double layer capacity which falls from 100 to 16 μF cm^{-2}. The low frequency capacitive loop is also consistent with the existence of an inhibiting process.

At point B_2 where the cathodic current is higher than at point B_1, the transfer resistance is lower. In addition the low frequency capacitive loop in plot B_2 leads to the domain of negative resistances, in agreement with the polarization curve which presents a negative slope in this region of potentials. Just past the current peak visible at -1.42 V, the low frequency capacitive loop returns to the quadrant corresponding to positive resistances.

Impedance plots also confirm the activating influence of the electrode excursion in the anodic domain upon the interfacial processes. Over the whole of the increasing part of the cathodic curve, the diagrams exhibit a shape similar to diagram B_1 but they reveal, as exemplified in diagram C, a considerable decrease in the values of the transfer resistance and polarization resistance. The capacity values deduced from the high frequency loop (400 μF cm^{-2}) are higher than at point A, in agreement with an increased electrode area consequent on the corrosion process.

Diagram D has been obtained in the polarization domain where the hydrogen evolution is passivated. In this plot the low frequency limit is only 0.06 Hz due to a slow drift of the electrode state, appearing as a decrease in the current density with electrolysis time. Three capacitive loops appear below 60 Hz and the one with lowest-frequency suggests a zero-frequency extrapolation with negative real parts, in reasonable agreement with the negative slope of the polarization curve at point D. These capacitive loops indicate that three distinct relaxation processes probably participate in the complex passivation process of hydrogen evolution on the electrode. As a normal consequence of the passivation process, the transfer resistance at point D is higher than at point C.

With a stationary electrode, the phenomena visible on polarization curves (Fig. 3) are similar to those observed with the rotating disc electrode. However zinc deposition is partly diffusion controlled, as seen on plot A′ in Fig. 4, where the small capacitive loop at low frequencies is due to the mass transfer interference with the interfacial processes. On the other hand, as a consequence of a better stability of steady states in the passivation domain than with the rotating electrode, the capacitive loop leading to a negative resistance is more visible on plot D′ in Fig. 4 than on plot D in Fig. 2. In addition from a comparison of Figs 1 and 3, it appears that the potential domain in which the

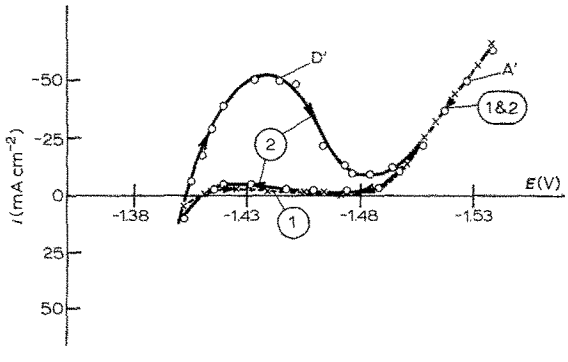

Fig. 3. Potentiostatic polarization curves with a stationary electrode. The electrolyte and plotting conditions are the same as for Fig. 1.

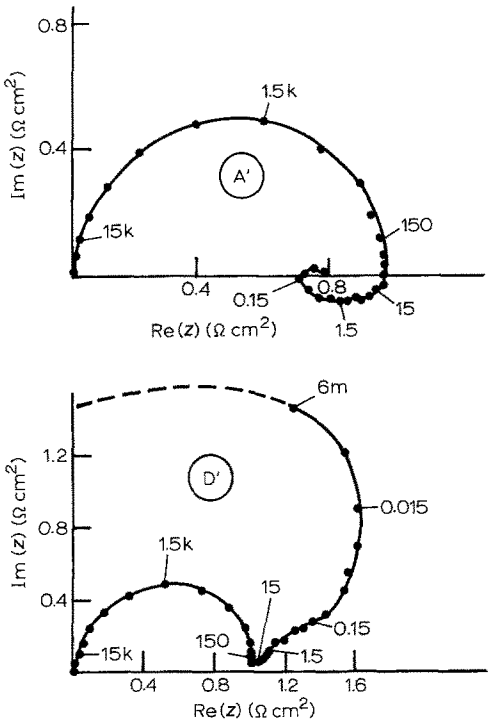

Fig. 4. Complex plane impedance plots obtained at point A′ and D′ in Fig. 3. Frequencies in Hz.

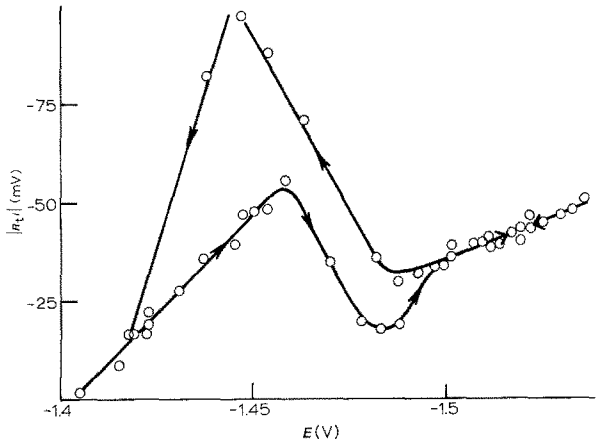

Fig. 5. Variation of the product of the transfer resistance, R_t, and current density, i, with the electrode potential. The arrows indicate the direction of potential variation.

electrode remains blocked is somewhat restricted in the case of natural convection (-1.41 to -1.48 V in Fig. 3). This result supports the idea that the electrolyte impurities are not the only adsorbed species responsible of the electrode passivation, since the electrode blocking largely subsists even with the motionless electrode for which the diffusion controlled amount of codeposited impurities is considerably reduced.

The potential dependence of the electrode behaviour is also apparent in Fig. 5 which represents the variation of the product of the transfer resistance, R_t, and current density, i, as a function of the electrode potential E, the corrosion potential E_{corr} being -1.403 V. At low cathodic polarization ($E > -1.45$ V) the linear relationship $|R_t i| = |E - E_{corr}|$ obtained with increasing polarization conforms to the classical behaviour of a fast system when the Butler-Volmer law governing the anodic and cathodic processes has been linearized near the equilibrium potential [10, 11] or the mixed potential of the system. At high polarization ($E < -1.49$ V) the slight dependence of $R_t i$ upon the electrode polarization indicates a nearly irreversible process for zinc deposition. The transition between these two domains occurs with hysteresis, the high values of the product $|R_t i|$ obtained with decreasing electrode polarization corresponding to a highly blocked electrode on which the cathodic reactions are hardly activated.

Some of the results presented in this paper can be explained on the basis of the model proposed by Epelboin *et al.* [1, 2]. In particular the inhibition of zinc deposition observed on curves 1 in Figs 1 and 3 can be ascribed to the adsorbed hydrogen. Then the reversible electrode activation occurring at high cathodic overpotentials implies the removal of this blocking adsorbate. According to this model, with increasing cathodic overpotential the adsorbed hydrogen is progressively replaced by the Zn^+_{ads} species which are involved in the autocatalytic mechanism for zinc electrodeposition.

At the corrosion potential, the dissolution process cleans the electrode surface which behaves as a freshly polished electrode surface. In the ascending branch of the hysteresis region hydrogen evolves on a permanently renewed and inhibitor-free zinc surface. With increasing overpotential both the corrosion and gas evolution processes vanish because of a progressive electrode passivation possibly due to Zn^+_{ads} whose surface concentration increases. Consequently, in agreement with a previous suggestion of hydrogen inhibition by adsorbed zinc ions or zinc atoms [14], it appears that zinc deposition occurs in highly acidic sulphate electrolyte when the hydrogen evolution is passivated by adsorbates, such as Zn^+_{ads}.

3.2. *Influence of nickel*

Curve 1 in Fig. 3, obtained with a fresh electrolyte and characterized by a current plateau corresponding to a quasi-blocked electrode, is not modified with the addition of a low concentration of nickel ions (between 0.1 and 5 mg l^{-1}). But after using the electrolyte for 10 to 12 h, the hysteresis observed when starting from point S is amplified even though the electrode polarization remains cathodic and it strongly depends upon the value at which the potential is reversed, as exemplified in Fig. 6. In this figure it is seen that the less cathodic reversing potential the higher the current peak obtained on the reverse curve. This is also true for the current minimum observed near -1.50 V. Such enhanced cathodic currents, as compared with Fig. 3, appear simultaneously with numerous electrogenerated gas bubbles and also with the deposit attack. Consequently even though the electrode potential remains in the cathodic domain, nickel traces activate both the hydrogen evolution and the zinc dissolution processes. The ascending cathodic branch corresponding to zinc

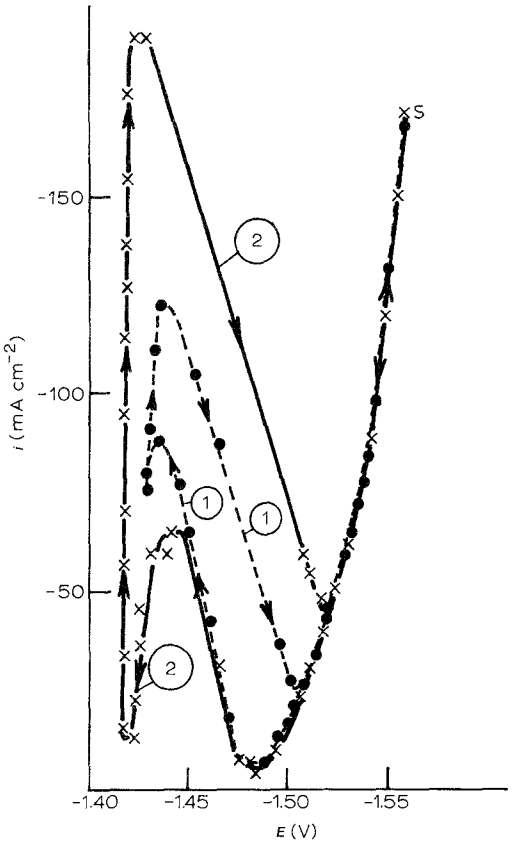

Fig. 6. Potentiostatic polarization curves plotted with a stationary electrode and two different reversing potentials: -1.43 V (curve 1); -1.42 V (curve 2). Electrolyte: 120 g l^{-1} H_2SO_4; 55 g l^{-1} Zn^{2+}; 4.9 mg l^{-1} Ni^{2+}.

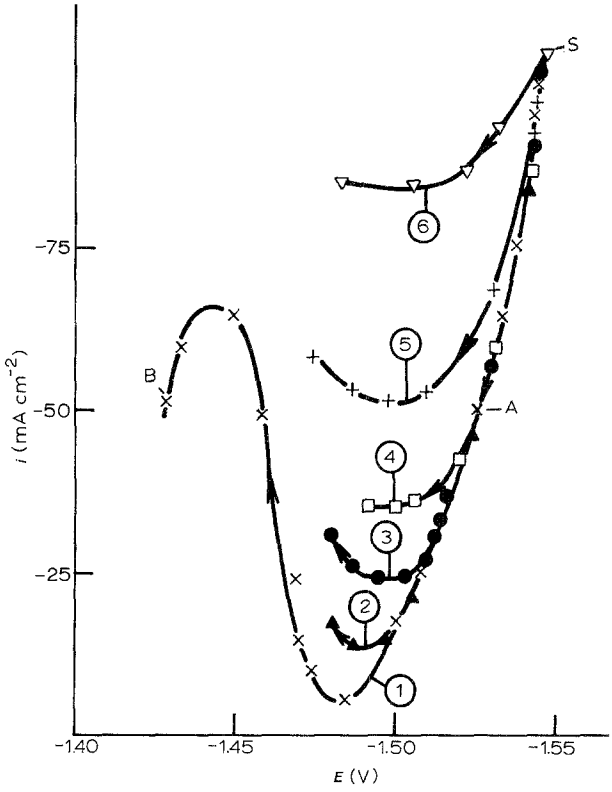

Fig. 7. Variation of the potentiostatic polarization curves with electrolysis time: 1 h (curve 1); 3 h (curve 2); 4 h (curve 3); 4.5 h (curve 4); 5.5 h (curve 5); 6.5 h (curve 6). Same electrolyte as for Fig. 6. Stationary electrode with a scratch.

deposition remains unchanged only between -1.52 and -1.56 V.

When a defect has been created on the electrode surface (e.g. a scratch), a time dependence of the polarization curve only appears in the case of nickel-containing electrolytes (Fig. 7). The current minimum apparent on curves plotted from point S progressively increases with time, thus showing that the inhibition of hydrogen evolution vanishes as nickel accumulates on the electrode surface. This progressive nickel accumulation destabilizes the electrochemical system even though the polarization remains very cathodic, i.e. $E < -1.48$ V. In Fig. 7, it clearly appears that under galvanostatic conditions, the steady-states corresponding to zinc deposition on the most cathodic branch progressively become unstable. For example, at a current density (c.d.) of 50 mA cm^{-2}, commonly used in zinc electrowinning [8], the steady-state corresponding to point A does not exist after ~ 5 h of electrolysis, and the only possible steady-state at this c.d. is point B. Accordingly the electrode will move from a state where hydrogen evolution and zinc deposition are predominant (point A) to a state where electrode corrosion takes place (point B).

With a scratched electrode and a higher concentration of Ni^{2+} in the electrolyte, decreasing the electrode polarization from point S leads randomly to various curves, as exemplified in Fig. 8. Hydrogen evolution and the deposit corrosion appear after a variable time-lapse, always shorter than for low Ni^{2+} concentrations.

The results of the present study with Ni^{2+} in the electrolyte confirm that a scratch on the electrode

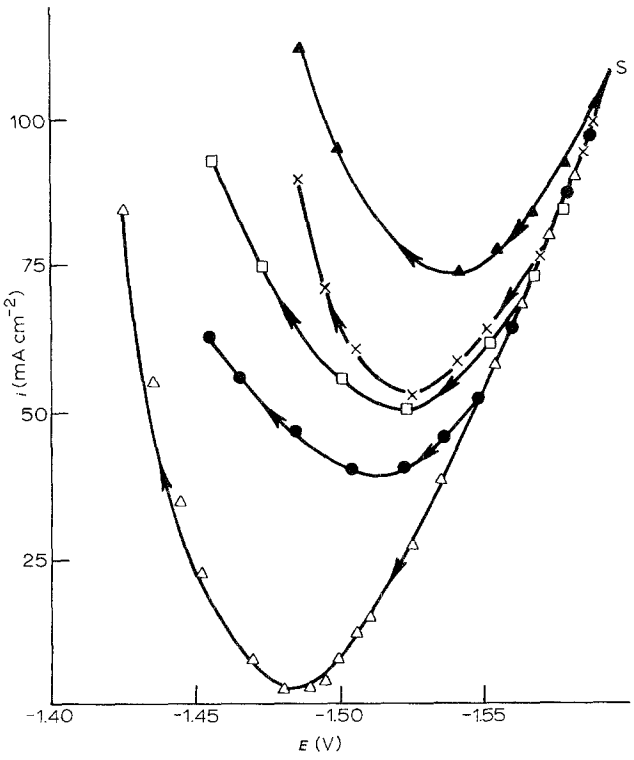

Fig. 8. Examples of potentiostatic curves obtained under identical experimental conditions, from point S, with the electrolyte: 120 g l^{-1} H_2SO_4; 55 g l^{-1} Zn^{2+}; 90 mg l^{-1} Ni^{2+}. Stationary electrode with a scratch.

surface plays a predominant role in the destabilization process of a stationary electrode, in agreement with previous observations [3, 8]. This destabilization process is due to the formation of local cells, initiated in the vicinity of surface defects (e.g. a scratch) where nickel can accumulate during zinc deposition. The presence of attached bubbles on such a defect can progressively isolate a local region of the interface from the bulk electrolyte, thus creating a destabilizing local cell. This mechanism is consistent with two experimental observations: (i) the zinc dissolution process starts precisely on the defect (scratch or pit) covered by attached bubbles [3, 8]; (ii) the electrolyte stirring releases the bubbles from the electrode surface and renders the destabilization more difficult [8, 12, 13].

4. Conclusion

In highly acidic sulphate electrolytes, it has been shown that zinc deposition implies a passivation process of hydrogen evolution on the deposit surface, possibly due to the intermediate Zn^{+}_{ads}.

The formation of local cells associated with the corrosion of zinc deposits can be provoked by an electrode excursion near the corrosion potential which depassivates the electrode. The presence of nickel in the electrolyte triggers the depassivation even though the electrode remains polarized in the cathodic domain. This depassivation occurs more easily at more cathodic potentials when a defect (a scratch) is previously formed on the substrate surface, especially in the case of a stationary electrode.

According to these results, it is clear that the problem of electrode destabilization by nickel impurities arises only with a galvanostatic control device able to generate multiple steady-states. Electrolyte stirring, a carefully polished substrate, and the use of a high deposition current density therefore appear to be beneficial in rendering this destabilization less likely.

Acknowledgements

The authors are indebted to Professor S. Rashkov and to C. Bozhkov, from the Bulgarian Institute of Physical Chemistry in Sofia, for helpful discussions on this research.

References

[1] I. Epelboin, M. Ksouri and R. Wiart, *J. Electrochem. Soc.* **122** (1975) 1209.
[2] *Idem, Faraday Disc. Chem. Soc.* No. **12** (1978) 115.
[3] M. Maja, N. Penazzi, R. Fratesi and G. Roventi, *J. Electrochem. Soc.* **129** (1982) 2695.
[4] T. J. O'Keefe, S. F. Chen, E. R. Cole Jr. and M. Dattilo, *J. Appl. Electrochem.* **16** (1986) 913.
[5] Y-M. Wang, T. J. O'Keefe and W. J. James, *J. Electrochem. Soc.* **127** (1980) 2589.
[6] D. J. Mackinnon and J. M. Brannen, *J. Appl. Electrochem.* **16** (1986) 127.
[7] C. Bozhkov, M. Petrova and S. Rashkov, *ibid.* **20** (1990) 11, 17.
[8] R. Wiart, C. Cachet, C. Bozhkov and S. Rashkov, *ibid.*, **20** (1990) 381.
[9] E. J. Frazer, *J. Electrochem. Soc.* **135** (1988) 2465.
[10] A. J. Bard and L. R. Faulkner, 'Electrochimie-Principes, methodes et applications', Masson (1982) p. 122.
[11] K. J. Vetter, 'Electrochemical Kinetics – Theoretical and Experimental Aspects', Academic Press, New York (1967) p. 154.
[12] D. J. Mackinnon, R. M. Morrison and J. M. Brannen, *J. Appl. Electrochem.* **16** (1986) 53.
[13] A. R. Ault and E. J. Frazer, *ibid.* **18** (1988) 583.
[14] T. Biegler, in 'Application of Polarization Measurements in the Control of Metal Deposition', (edited by I. H. Warren), Elsevier Science Publishers, Amsterdam (1984) p. 32.